

formed as previously described (5), except that pancreata from obese Zucker females and Zucker diabetic fatty males were subjected to a second 16-min collagenase digestion using half strength (0.25%) collagenase before Ficoll purification of islets. This was necessary because of the increase in fibrous tissue in both groups. The uptake of 3-O-methyl- β -D-glucose and L-glucose was measured as previously described (5).

13. Anti-GLUT-2 antibody #1092 was raised against COOH-terminal hexadecapeptide RKATVQME-FLGSSETV predicted from the DNA sequence of GLUT-2 (10) and synthesized by S. Stradley and L. Gierasch, University of Texas Southwestern Medical Center. The peptide was coupled to purified protein derivative (PPD) by the method of Lachmann *et al.* [P. J. Lachmann, L. Strangeways, A. Vyakarnam, G. Evan, in *Synthetic Peptides as Antigens*, R. Porter and J. Whelan, Eds. (Ciba Foundation Symposium, 1986), vol. 119, pp. 25–57] and was injected with Freund's complete adjuvant subcutaneously into New Zealand white rabbits. Rabbits were boosted after 6 weeks with PPD-coupled peptide suspended in Freund's incomplete adjuvant. Crude islet membrane preparations were made by homogenizing whole islets suspended in 50 mM Hepes, pH 7.4, 250 mM sucrose, 1 mM EDTA, and 1 mM trasyolol with 20 strokes of a Teflon-glass Potter-Elvehjem homogenizer (14). After centrifugation at 25,000g for 20 min at 4°C, the sediment was resuspended in homogenizing buffer, layered over 40% sucrose, and centrifuged at 150,000g for 2 hours at 4°C in an SW 41 rotor. After harvesting the crude membranes from the 40% sucrose–overlay interface the membranes were resedimented and solubilized in the appropriate amount of digestion buffer for SDS–polyacrylamide gel electrophoresis [U. K. Laemmli, *Nature* 227, 680 (1970)]. Following electrophoresis and electrotransfer to nitrocellulose filters (Bio-Rad), the filters were blocked with 10 mM Tris, pH 7.4, 0.15 mM NaCl, 10 mM EGTA, 0.1% Tween 20, and 5% bovine serum albumin (BSA). The filters were incubated at room temperature for 2 hours in the above buffer containing 0.5% BSA and a 5×10^4 dilution of rabbit antibody against rat GLUT-2, washed and developed with 10^6 cpm/ml 125 I goat Fab antibody to rabbit immunoglobulin G.
14. L. Chen *et al.*, *Proc. Natl. Acad. Sci. U.S.A.* 87, 4088 (1990). All pancreata were perfused with 4% paraformaldehyde and 0.05% glutaraldehyde. Frozen tissue sections were hybridized [D. M. Simmons, J. L. Arizza, L. W. Swanson, *J. Histochem. Technol.* 12, 169 (1986)] with 5×10^6 dpm/ml of 35 S-labeled antisense GLUT-2 RNA in 50% formamide at 55°C overnight. After ribonuclease treatment and washing under stringent conditions, the slides were dipped in Kodak NTB-3 emulsion and exposed in the dark for 1 week. Density of GLUT-2 mRNA hybridization was measured with the use of the spot meter of a Nikon microscope photographic VFXIIIA system at constant light setting and ASA 100. Reciprocals of reading exposure time of individual islets in dark-field image were used to represent the signal grain density after correcting for the background. Twenty randomly picked islets from each group of rats were measured.
15. L. Orci, B. Thorens, M. Ravazzola, H. F. Lodish, *Science* 245, 295 (1989).
16. The curve in Fig. 4A was linearized to obtain the slope. The equation of the curve is $y = 824.1 \times 10^{-0.0084x}$, where y is plasma glucose and x is percentage of GLUT-2-positive β cells. In linearized form, this is $\log_{10} y = 2.916 - 0.0084x$.
17. We thank M. S. Brown, D. W. Foster, and K. L. Luskey, for reading this manuscript, R. Risser, for statistical analyses, T. Autrey for excellent secretarial work and K. McCorkle for expert technical assistance. Supported by NIH grant DK02700-30, Veterans Administration Institutional Research Support grant 549-8000, Research and Education Foundation, Juvenile Diabetes Foundation grant 187417, Swiss National Science Foundation grant 31-26625.89, American Diabetes Association Research and Education Foundation, American Heart Association–Texas affiliate.

8 May 1990; accepted 14 August 1990

Involvement of the Silencer and UAS Binding Protein RAP1 in Regulation of Telomere Length

ARTHUR J. LUSTIG,* STEPHEN KURTZ, DAVID SHORE

The yeast protein RAP1, initially described as a transcriptional regulator, binds *in vitro* to sequences found in a number of seemingly unrelated genomic loci. These include the silencers at the transcriptionally repressed mating-type genes, the promoters of many genes important for cell growth, and the poly[(cytosine)_{1–3} adenine] [poly(C_{1–3}A)] repeats of telomeres. Because RAP1 binds *in vitro* to the poly(C_{1–3}A) repeats of telomeres, it has been suggested that RAP1 may be involved in telomere function *in vivo*. In order to test this hypothesis, the telomere tract lengths of yeast strains that contained conditionally lethal (*ts*) *rap1* mutations were analyzed. Several *rap1^{ts}* alleles reduced telomere length in a temperature-dependent manner. In addition, plasmids that contain small, synthetic telomeres with intact or mutant RAP1 binding sites were tested for their ability to function as substrates for poly(C_{1–3}A) addition *in vivo*. Mutations in the RAP1 binding sites reduced the efficiency of the addition reaction.

THE TELOMERES OF ALL EUKARYOTES examined thus far consist of a guanine-cytosine (GC)-rich sequence of variable length [for example, poly(C_{1–3}A) in *Saccharomyces cerevisiae*] (1). The G-rich strand appears to be added in a DNA template-independent process that requires telomerase, a ribonucleoprotein (2). In several organisms, the sequences present at telomeres are organized into an altered chromatin structure that is resistant to degradation by micrococcal nuclease (3, 4). In yeast and ciliates, nonhistone proteins that bind telomere sequences have been identified (4, 5). The interaction of these proteins with telomeric DNA is likely to be important for the control of telomere replication, association, and higher order structure (1).

In *S. cerevisiae*, the predominant telomere-binding protein is RAP1 (also known as TBA, GRF1, and TUF1) (5–7). Telomeric binding sites for RAP1 [ACACCCA-CACACC] are found at an average density of one site per 40 bp of telomeric poly(C_{1–3}A) (8, 9). The gene encoding RAP1 has been cloned and is essential for viability (7).

To investigate whether RAP1 affects telomere structure *in vivo*, we analyzed chromosomal telomere lengths in four independent *rap1^{ts}* mutants. Each mutant allele was a unique recessive missense mutation and displayed a distinct pattern of growth. Strains that contained the *rap1-2* or *rap1-5* alleles grew at or near wild-type rates under permissive conditions (23°C) and required at

least 16 hours of incubation at the restrictive temperature (37°C) to inhibit growth. Strains that carried either the *rap1-1* or *rap1-4* alleles grew poorly at 23°C and rapidly arrested growth when shifted to 37°C.

The effect of the *rap1^{ts}* mutations on the size of telomeric poly(C_{1–3}A) tracts was analyzed by culturing each mutant strain at permissive or semipermissive temperatures for approximately 100 generations. The semipermissive temperature was defined as the temperature at which a significant decrease in growth rate occurred. Under these conditions, cells were partially deficient in RAP1 activity. The tract length of the predominant class of telomeres (the XY' class, see Fig. 1A) was measured by hybridizing Southern (DNA) blots of Xho I-digested genomic DNA with 32 P-labeled poly[d(GT)]·poly[d(CA)], which identified the telomeric poly(C_{1–3}A) sequences and internal poly(CA) tracts (Fig. 1A).

At the permissive temperature (23°C), telomeres showed only minimal alterations in tract length (Fig. 1B). However, at semipermissive temperatures (30° to 31.5°C), telomere tract size was gradually reduced in *rap1^{ts}* cells during ~100 generations of culturing (300 to 125 bp, Fig. 1C). Progressive loss of sequences, observed in both *rap1-2* mutant haploids and homozygous diploids, was recessive; diploids that were heterozygous for the *rap1-2* mutation had wild-type tract lengths (10). Strains containing either the *rap1-4* or the *rap1-1* allele showed a moderate loss of telomeric sequences (~130 and ~88 bp, respectively) when cultured at 23°C (10). No significant changes in telomere sizes were observed in isogenic wild-type strains at any of the temperatures used in this study (Fig. 1, B and C).

The loss of terminal tracts observed in *rap1-2* mutants was fully reversible. When

A. J. Lustig, Department of Molecular Biology, Memorial Sloan-Kettering Cancer Center, New York, NY 10021.

S. Kurtz and D. Shore, Department of Microbiology, College of Physicians and Surgeons, Columbia University, New York, NY 10032.

*To whom correspondence should be addressed.

cells that were subcultured four times at 31.5°C were returned to the permissive temperature, wild-type telomere tract size was regained after several rounds of subculturing (Fig. 2). These data indicate that no permanent change in telomere structure occurred during the subculturing procedure.

Strains that contained the *rap1-5* allele displayed a more complex phenotype (Fig. 3). At 23°C, both the average size of telomere tracts and the degree of tract size heterogeneity were increased relative to wild-type telomeres. However, at 31.5°C the average tract length decreased during subculturing and reached a new tract length that was 50 to 100 bp shorter than the tract length in wild-type cells.

It is unlikely that the observed changes in tract lengths resulted from a decrease in growth rate in the ts mutants. First, growth of wild-type cells in nutrient-limiting condi-

tions reduced growth rate, but did not affect telomere length. Second, the allele specificity we observed argues against a nonspecific cause for telomere tract loss. For example, *rap1-1* mutants had a growth rate at 23°C that was comparable to the growth rate of *rap1-2* mutants at 31.5°C, yet telomere tract loss in the *rap1-1* strain was much less extensive than that observed for *rap1-2*. Finally, *rap1-5* mutants had elongated telomeres at the permissive temperature, at which the growth rate of these mutant cells was minimally impaired. These observations suggest that RAP1 affects telomere structure in a complex fashion.

The changes in telomeric length observed in the *rap1* mutants also occurred in the X class of telomeres (Fig. 1A). In contrast, no changes in the sizes of fragments of nontelomeric poly(CA) tracts were observed. It is therefore unlikely that the changes in telomere length resulted from rearrangement of Y' sequences. Telomere lengths in all of the *rap1* mutants stabilized at new tract sizes and did not change continuously. It is not clear

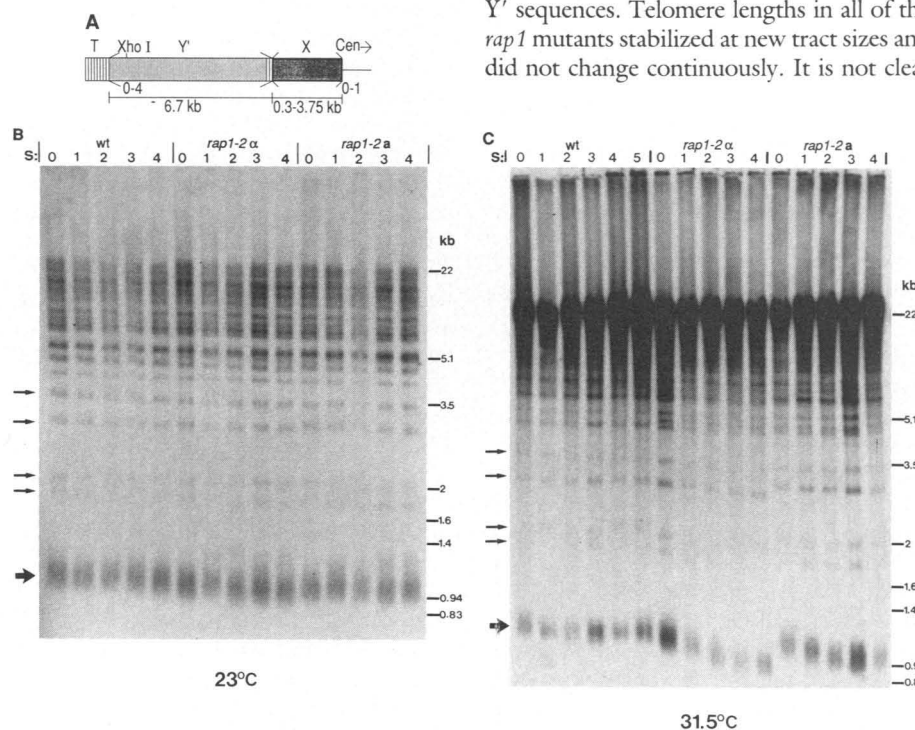


Fig. 1. *rap1^{ts}* mutants alter telomere length. **(A)** The organization of sequences at the yeast telomere. The telomere (T, bars) consists of poly(C₁₋₃A) sequences oriented 5' to 3' toward the centromere (Cen). Most chromosomes have two subtelomeric repeated sequences. Y' (light screen) and X (dark screen). The Y' element contains an Xho I endonuclease site ~1.3 kb from the end of the telomere. Southern analysis of Xho I-digested chromosomal DNA with the probe poly[d(GT)]·poly[d(CA)] reveals a ~1.3-kb signal, which represents the telomere class containing both X and Y' elements (XY' class telomeres; large arrows in Figs. 1 to 3), as well as internal sequences (24). Chromosomes lacking the Y' element (X class telomeres) display a different pattern of hybridization after Xho I digestion (small arrows in Figs. 1 to 3). The lengths of the telomeric tract are deduced from the center of distribution of the telomeric XY' Xho I fragments as described (11, 17). **(B and C)** Southern blots of Xho I-digested DNA isolated from both wild-type (wt) and *rap1-2* mutant strains were probed with poly[d(GT)]·poly[d(CA)]. For these experiments, DNA was isolated after each of four to five subsequent subculturings on solid media at either 23°C (B) or 31.5°C (C), as described (11). Each round of subculturing represented ~25 generations of growth. Lane designations: S, number of rounds of subculturing; 0, initial culture; 1 to 4 and 1 to 5, four and five subculturings, respectively. Size markers (λ genomic DNA digested with Eco RI and Hind III) are shown at the right. At 23°C, only a small amount of tract loss (~60 to 80 bp) from the wild-type tract size of 280 bp was observed in mutant cells. The apparent difference in tract length between the *MATa* (loss of ~150 bp) and *MATα* (loss of ~200 bp) derivatives of the *rap1-2* strain at 31.5°C was eliminated upon further subculturing. The *rap1^{ts}* mutations were derived as described (25).

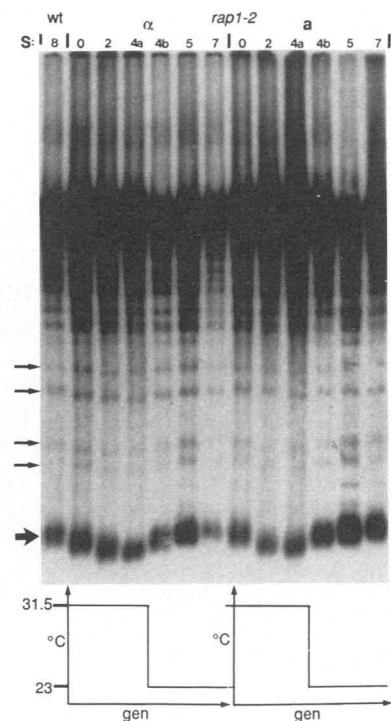


Fig. 2. Southern (DNA) blot analysis of wild-type (wt) and *rap1-2* mutant strains after a shift from 31.5°C to 23°C. Wild-type cells and both *MATa* and *MATα* derivatives of the *rap1-2* strain were subcultured four times at the semipermissive temperature (31.5°C), after which the culture was returned to the fully permissive temperature (23°C) for four more rounds of subculturing. DNA was then analyzed as described in the legend to Fig. 1. Lane designations indicate subculturations (defined in the legend to Fig. 1) at 31.5°C (s: 0 to 4a) and then at 23°C (s: 4b to 7). Lanes marked 4a and 4b denote growth for less than a full round of subculturing. The line drawing below the blot indicates the point at which the temperature was shifted and corresponds to the samples on the gel. The wild-type DNA (the S8 designation) was derived from the last of four subculturations at 23°C. Size standards and arrows are as described in the legend to Fig. 1.

whether this effect is the consequence of a new steady state between activities that add and delete terminal tract sequences (11) or the accumulation of suppressors of the telomere phenotype. *RAP1* is not allelic to any previously identified mutations that affect telomere structure in yeast (11, 12). Of all the mutations known to affect telomere tract length, the ts mutations in *RAP1* described herein are the first such mutations in a gene whose product is known to bind telomere sequences in vitro.

The phenotype of the *rap1^{ts}* mutants and the occurrence of *RAP1* binding sites in the poly(C₁₋₃A) repeats of telomeres suggest that *RAP1* binds at telomeres in vivo and affects their function. We tested this idea further by constructing several artificial telomeres that contained either wild-type *RAP1* binding sites or mutated sites impaired in their ability to bind *RAP1*. These artificial

telomeres were linked to the termini of a replicating plasmid and transformed into yeast (Fig. 4B). The structure of plasmids recovered from transformants was compared with the structure of the initial transforming plasmid (Fig. 4A). During transformation, plasmids may be modified (healed) by the addition of poly(C₁₋₃A) sequences onto telomere-like substrates, thereby allowing their propagation as linear molecules (9, 13). This assay has been used to show that telomeres from ciliates and humans function as substrates for poly(C₁₋₃A) addition (14). Thus, this telomere healing assay serves as a model for chromosomal telomere addition, although it may reflect the outcome of a number of processes that involve telomeres in vivo.

Artificial telomeres were constructed and tested for RAP1 binding in a gel mobility shift assay (Figs. 4 and 5A). The wild-type telomere (AT1) was a 41-bp sequence designed on the basis of the yeast telomere

consensus sequence poly[C₂₋₃A(CA)₁₋₃] (15) and contained two perfect matches to the telomeric form of the RAP1 binding site (ACACCCACACACC) as well as a third overlapping 12/13 nucleotide match (Fig. 4B). RAP1 bound efficiently to this artificial telomere and, as expected from the size of the RAP1 footprint (7, 16), apparently occupied the two nonoverlapping sites (Fig. 5A). Two mutant telomeres, AT5 and AT12, contained changes in the central regions of all three potential RAP1 binding sites and bound RAP1 poorly (AT5) or not at all (AT12). Another telomere, AT13, contained only a single RAP1 binding site, which had a 12/13 nucleotide match to the binding site consensus sequence. AT13 had a reduced binding affinity relative to AT1 and to other probes that contained high-affinity RAP1 binding sites (10). Neither AT5, AT12, nor AT13 effectively compete with AT1 for the binding of RAP1 (Fig. 5B). In contrast, the telomere AT16, which

contained three nucleotide changes in positions not expected to affect RAP1 binding, bound efficiently to RAP1.

After transformation with Bam HI-linearized AT1 plasmids, most transformants contained linear plasmids that had undergone poly(C₁₋₃A) addition (transformants that contained healed linears, HL_T) onto both artificial telomeres (92% HL_T) (Table 1). These plasmids had telomeric tract sizes comparable in length to chromosomal telomeres (360 ± 180 bp) (10, 17). Linear recombinant and circular recombinant plasmids were recovered in the small number of the transformants that lacked HL forms (5 and 2%, respectively).

In contrast, after transformation with Bam HI-linearized AT5, AT12, or AT13 plasmids, a reduced percentage of recovered transformants that contained HL forms was observed (17.5, 31.5, and 22.5%, respectively) (Table 1). Unlike the case of AT1, the plasmids recovered from AT5, AT12, and AT13 transformants were predominantly recombinant forms. Transformants with AT12 also showed an increased frequency of linear plasmid species that contained a longer tract (>650 bp) on one or both arms of the plasmid (aberrant linear) (Table 1). Although the magnitude of this increased frequency varied among experiments, the addition of large terminal tracts is only rarely observed in wild-type AT1 telomeres (1 out of 212 analyzed). This effect probably resulted from a greater than normal amount of poly(C₁₋₃A) added in the initial events after transformation. For AT16, which bound efficiently to RAP1 in vitro, a high percentage of normal plasmid healing was observed (84% HL_T forms) (Table 1).

These data suggest that strong RAP1 binding sites (AT1 and AT16) are important for the efficiency and fidelity of plasmid healing and further support the idea that RAP1 acts in a direct manner to affect telomere structure. Reduction in RAP1 binding affinity roughly correlated with reduced plasmid healing. However, we did not observe a strict correlation between the affinity of binding and the degree of plasmid healing and it is conceivable that these mutations also affected other aspects of telomere healing. Mutations in the RAP1 binding sites may affect the efficiency of telomere addition or may increase recombination or degradation. We do not yet know whether the decrease in healing efficiency observed with mutated RAP1 binding sites is due to loss of RAP1 binding in vivo.

On the basis of the genetic experiments described above, we suggest that RAP1 has a direct effect on regulating telomere length in vivo. Recent evidence demonstrating that intragenic suppressors of *rap1-5* lethality

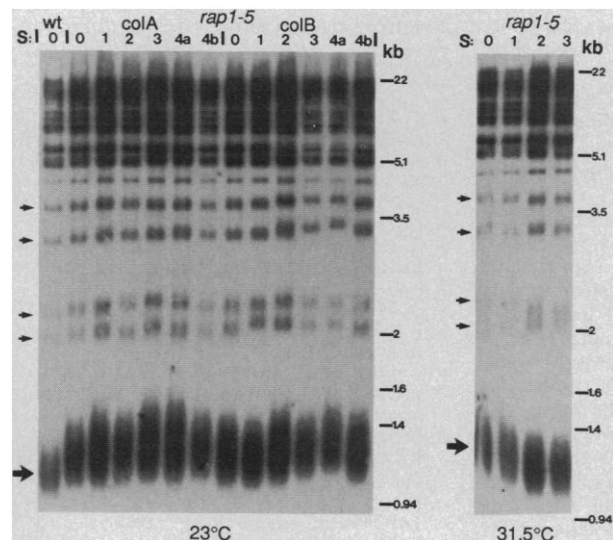
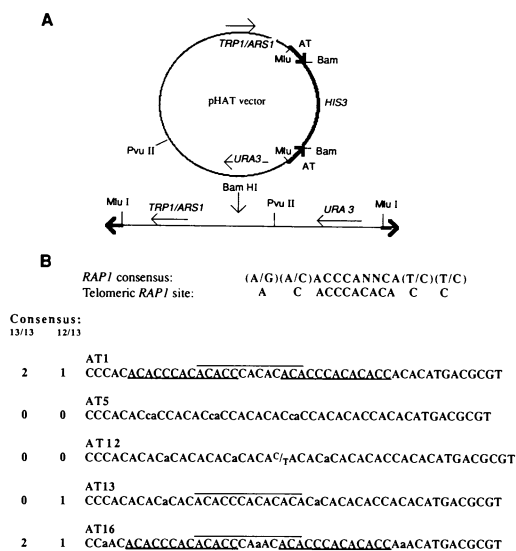


Fig. 3. Southern analysis of the *rap1-5* strain after four subculturings at 23°C (left panel, S: 0 to 4) or three subculturings at 31.5°C (right panel, S: 0 to 3) (see the legend to Fig. 1). DNA was isolated and characterized as described in the legend to Fig. 1. For the 23°C subculturing, two colonies (colA and colB), independently derived from single cells, were examined. For the 31.5°C subculturing, only the results from colony B are shown. In the left panel, the lanes marked 4a and 4b refer to two colonies taken from the fourth subculturing plate. A wild-type (wt) control is shown in the left panel. Size standards and arrows are as in Fig. 1.

Fig. 4. (A) Construction of artificial telomeres (26). Plasmids that contained the structures shown were termed pHAT. These vectors contained YRp17 flanked by the artificial telomeres. (B) The sequences of the telomeres used in this study and the telomeric binding site for RAP1. The CA-rich strand, oriented 5' to 3', is shown. In each case, 41 bp of telomeric sequence are adjacent to 12 nucleotides of additional sequence. The underlines and the overline indicate the perfect matches and the overlapping 12/13 match, respectively, to the consensus RAP1 binding site that are present in AT1 and mutant telomeres. The number of perfect and 12/13 matches to the consensus sequence present in each telomere is shown on the left. Mutations are indicated in lowercase letters. Telomeres of the pHAT plasmids were sequenced directly and, with two exceptions, were as expected (27).



contain telomeres up to 4 kb longer than those of wild-type cells is consistent with this hypothesis (18). How can a transcriptional regulatory protein also function in maintaining telomere structure? One explanation for the apparent multifunctional nature of RAP1 is its participation in the formation of altered chromatin structure. Consistent with this proposal is the presence of a unique region of yeast telomeric chromatin, which is resistant to micrococcal nuclease digestion (3). Similarly, chromatin at the silent mating-type loci is more resistant to nuclease digestion than that at the expressed *MAT* locus (19). Furthermore, silencing requires the highly conserved NH₂-terminus of histone H4, again suggesting a role for modified chromatin structure in this process (20). The silent loci are refractory to cutting by the HO endonuclease, switching of the mating-type information, and transcription (21). These observations, together with the recent finding that normally constitutive genes become repressed when located near telomeric sequences (22), suggest that RAP1 may be involved in converting the silent mating-type loci and telomeres into a protected, heterochromatic state.

Another clue to the mechanism of RAP1 action comes from the observation that the protein fractionates with the nuclear scaffold (23). RAP1 may function by sequestering telomeres to particular regions of the nucleus either to facilitate the binding of telomere replication enzymes or to protect the telomere from degradation and recombination.

REFERENCES AND NOTES

1. V. Zakian, *Annu. Rev. Genet.* **23**, 579 (1990).
 2. C. Greider and E. Blackburn, *Cell* **43**, 405 (1985); *Nature* **337**, 331 (1989); A. Zahler and D. Prescott, *Nucleic Acids Res.* **16**, 6359 (1988); D. Shippen-Lentz and E. Blackburn, *Mol. Cell. Biol.* **9**, 2761 (1989); G. Morin, *Cell* **59**, 521 (1989).
 3. B. Dunn, thesis, Harvard University (1989); M. Budarf and E. Blackburn, *J. Biol. Chem.* **261**, 363 (1986).
 4. D. Gottschling and T. Cech, *Cell* **38**, 501 (1984).
 5. J. Berman, C. Tachibana, B.-K. Tye, *Proc. Natl. Acad. Sci. U.S.A.* **83**, 3713 (1986).
 6. J. Huet *et al.*, *EMBO J.* **4**, 3539 (1985); A. Buchman, W. Kimmerly, J. Rine, R. Kornberg, *Mol. Cell. Biol.* **8**, 5086 (1988).
 7. D. Shore and K. Nasmyth, *Cell* **51**, 721 (1987).
 8. B. Dunn, P. Szauter, M. Pardue, J. Szostak, *ibid.* **39**, 191 (1984); L. Button and C. Astell, *Mol. Cell. Biol.* **6**, 1352 (1986); R. Walmsley, C. Chan, B.-K. Tye, T. Petes, *Nature* **310**, 157 (1984).
 9. J. Shampay, J. Szostak, E. Blackburn, *Nature* **310**, 154 (1984).
 10. A. Lustig, S. Kurtz, D. Shore, unpublished data.
 11. A. Lustig and T. Petes, *Proc. Natl. Acad. Sci. U.S.A.* **83**, 1398 (1986).
 12. M. Carson and L. Hartwell, *Cell* **42**, 249 (1985); V. Lundblad and J. Szostak, *ibid.* **57**, 633 (1989); S. Kronmal and T. Petes, personal communication; A. Lustig and D. Shore, unpublished data.
 13. R. Walmsley, J. Szostak, T. Petes, *Nature* **302**, 84 (1983).
 14. A. Murray, T. Claus, J. Szostak, *Mol. Cell. Biol.* **8**, 4642 (1988); A. Pluta *et al.*, *Proc. Natl. Acad. Sci. U.S.A.* **81**, 1475 (1984); H. Riethman, R. Moyzis, J. Meyne, D. Burke, M. Olson, *ibid.* **86**, 6240 (1989); S. Cross, R. Allshire, S. McKay, N. McGill, H. Cook, *Nature* **338**, 771 (1989); W. Brown, *ibid.*, p. 774; J. Cheng, C. Smith, C. Cantor, *Nucleic Acids Res.* **17**, 6109 (1989).
 15. E. Blackburn, *Cell* **37**, 7 (1985).
 16. M. Longtine, N. Wilson, M. Petracek, J. Berman, *Curr. Genet.* **16**, 225 (1989).
 17. R. Walmsley and T. Petes, *Proc. Natl. Acad. Sci. U.S.A.* **82**, 506 (1985).
 18. A. Lustig, unpublished data.
 19. K. Nasmyth, *Cell* **30**, 567 (1982).
 20. P. Kayne *et al.*, *ibid.* **55**, 27 (1988).
 21. A. Klar, J. Strathern, J. Broach, J. Hicks, *Cell* **25**, 517 (1981); J. Strathern *et al.*, *ibid.* **31**, 183 (1982).

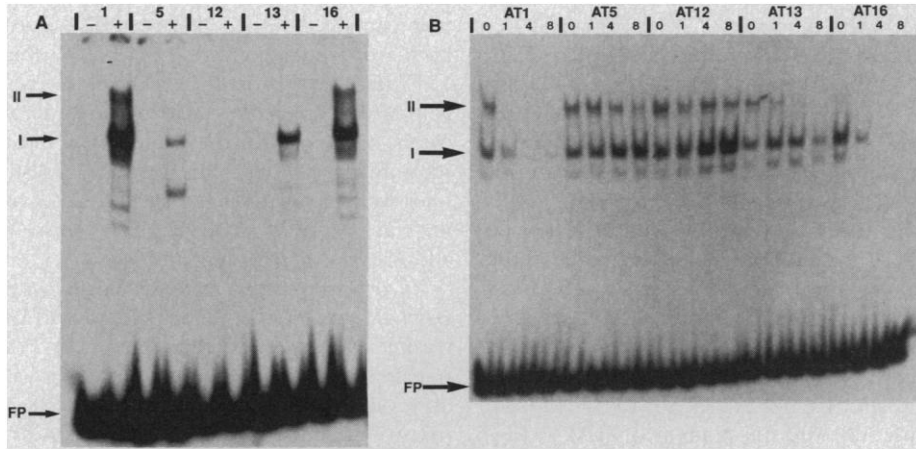


Fig. 5. Gel mobility shift assays performed with wild-type and mutant RAP1 binding sites (28). (A) Lane designations indicate the absence (-) or presence (+) of yeast extract in the binding reactions. The complexes formed were as follows: I, RAP1 bound at one site on the oligonucleotide; and II, RAP1 bound at two of the available sites on the oligonucleotide. FP indicates the free probe. Minor complexes that migrated faster than complex I were degradation products of RAP1 protein that retained DNA binding activity. (B) Gel mobility shift assay performed with ³²P-labeled AT1 and plasmid competitor DNA that contained each telomere oligonucleotide. Competitor DNA was present at 0, 100, 400, and 800 ng per reaction. Molar ratios of competitor to probe DNA are indicated above each lane.

Table 1. Products of transformations with artificial telomeres. The pooled results of all experiments in which identical amounts of Bam HI-digested artificial telomere plasmids (pHAT1, 5, 12, 13, or 16) were transformed into a *ura3* derivative of the strain A364A (29) by use of the spheroplast method (30). DNA levels varied from 0.26 to 0.41 μg in different experiments. A minimum of two transformations was done for each plasmid with both circular plasmids and Bam HI-digested pHAT1 included as controls. Calf thymus DNA (10 μg) was added as carrier in all transformations. The data are presented as percentages of plasmids having the following structures: healed linear, which are formed by the addition of poly(C₁₋₃A) to both plasmid termini; healed linear + recombinants, which are healed plasmids in the presence of additional recombinant forms; aberrant linears, which are healed linears with longer tracts (at least 300 bp greater than wild-type lengths) on one or both arms of the plasmid; linear recombinants, which consist of linear inverted dimers as well as more complex forms, and appear to arise from poly(C₁₋₃A) addition at one of the two ends and ligation or recombination at the other; and circular/complex recombinants, which consist primarily of recircularizations of the linearized plasmid, circular inverted dimers, and multimeric circular forms, as well as some structures that could not be determined due to their complexity or low abundance. Integration events were identified by a high level of mitotic stability not exhibited by extrachromosomal plasmids. Percentage of HL_T refers to transformants containing healed linears of normal structure and is the sum of the first two columns of the table. The number of trials for each construct and the cumulative sample size, respectively, are indicated in the parentheses below each telomere. A second trial for AT16, not shown here, was performed in a different strain with essentially identical results. Plasmid (31) and statistical analyses (32) were as described.

| Telomere (trials; events) | Transformation products (%) by class | | | | | | HL _T |
|---------------------------|--------------------------------------|------------------------------|-----------------|---------------------|-------------------------------|--------------------|-----------------|
| | Healed linear | Healed linear + recombinants | Aberrant linear | Linear recombinants | Circular/complex recombinants | Integration events | |
| AT1 (5;212) | 74.0 | 18.0 | 0.5 | 5.0 | 2.0 | 0.5 | 92.0 |
| AT5 (3;109) | 13.0 | 4.5 | 0.0 | 24.0 | 57.5 | 1.0 | 17.5 |
| AT12 (3;106) | 22.5 | 9.5 | 10.5 | 28.5 | 27.0 | 2.0 | 31.5 |
| AT13 (2;71) | 19.5 | 3.0 | 1.5 | 32.5 | 42.0 | 1.5 | 22.5 |
| AT16 (1;44) | 66.0 | 18.0 | 0.0 | 7.0 | 9.0 | 0.0 | 84.0 |

22. D. Gottschling, personal communication.
23. J. Hofmann, T. Laroche, A. Brand, S. Gasser, *Cell* 57, 725 (1989).
24. C. Newlon, *Microbiol Rev* 4, 568 (1988).
25. The *rap1^Δ* mutations were obtained by hydroxylamine mutagenesis of the cloned *RAP1* gene (S. Kurtz and D. Shore, in preparation). Mutant alleles were substituted for the wild-type copy of *RAP1* in the genome. Each mutation is recessive and segregates 2:2 in a cross with an isogenic wild-type derivative. Mutants were tested in a minimum of two independent experiments.
26. Telomeric tracts (60 ng) that contained a Bcl I cohesive end were prepared by annealing two complementary gel-purified oligonucleotides and were subsequently ligated to a Bam HI-linearized replicating plasmid, YRp17 (1 μg). The DNA was then ligated to a Bam HI fragment that contained the *HIS3* gene, the ends of which had been previously filled in with the Klenow fragment of DNA polymerase I, and transformed into the *Escherichia coli* strain HB101. The vectors obtained contained YRp17 flanked by artificial telomeres that were separated by the *HIS3* gene to avoid the rearrangement of inverted repeats in *E. coli* [A. Murray and J. Szostak, *Mol Cell Biol* 6, 3166 (1986)]. Because ligation of the *HIS3*-containing fragment to the artificial telomeres recreated the Bam HI site, digestion of this plasmid with Bam HI resulted in the formation of a YRp17 plasmid terminated by telomeric sequences. The sequences present at the plasmid termini were identical to those present in the original oligonucleotide with the exception of a 4-bp 5' overhang.
27. In the case of AT12, one of the two telomeric tracts (*URA3* proximal) contained an additional C to T change, designated by CT, outside of the two nonoverlapping *RAP1* binding sites. In the case of AT16, an apparent structural anomaly at the end of the *URA3* proximal telomere did not permit an accurate determination of the terminal 5 bp of this telomere.
28. D. Shore, D. Stillman, A. Brand, K. Nasmyth, *EMBO J*, 6, 461 (1987). Gel mobility shift assays were performed with 10 μg of total yeast extract prepared from cells expressing wild-type *RAP1* and oligonucleotides that contained the wild-type and mutant telomeres. Telomeres were labeled with [α -³²P]deoxyadenosine triphosphate and the Klenow fragment of DNA polymerase I by filling in the Bcl I overhang.
29. L. Hartwell, *J Bacteriol* 93, 1662 (1967).
30. F. Sherman, G. Fink, J. Hicks, *Methods in Yeast Genetics* (Cold Spring Harbor Laboratory, Cold Spring Harbor, NY, 1986).
31. For each transformation, a random collection of transformants was picked to ensure the absence of any bias (for example, colony size). Unpurified transformants were used so as to identify all products of the transformation event. DNA was isolated from these transformants and the structures of the plasmids were determined by the presence of extrachromosomal plasmids in blots of undigested DNA probed with either poly[d(GT)]-poly[d(CA)] or pBR322, and by digestion of the plasmids with Pvu II, which cuts once within the plasmids. Aberrant linear forms were initially identified by Pvu II digestion and confirmed by Mlu I digestion. In aberrant linear forms, terminal fragments varying in length, up to 1 kb longer than the usual 360-bp tract, were observed after digestion with Mlu I (data not shown). Recombinant structures were confirmed by more extensive restriction analyses in a subset of transformant DNAs.
32. D. Matthews and V. Farewell, *Using and Understanding Medical Statistics* (Karger, Basel, 1988), pp. 39–46. Statistical analyses of the relative frequencies of transformant products were carried out by contingency χ^2 analyses with expected values of 5 or greater. The minimum χ^2 value among individual experiments for the decrease of *HL₁* for AT5 is 16.7 ($P < 0.001$), for AT12 is 8.3 ($P < 0.005$), and for AT13 is 22 ($P < 0.001$). The minimum χ^2 value for the decrease of *HL₁* for AT5 is 37.9 ($P < 0.001$), for AT12 is 18.2 ($P < 0.001$), and for AT13 is 17.8 ($P < 0.001$). The χ^2 value for the differences between AT1 and AT16 in healed linears is 0.94 ($P < 0.3$), which is not statistically

significant. The decreases in the proportion of healed linears with the use of mutant telomeres are significant when compared with the AT1 control included in each experiment and when represented as cumulative data as shown in Table 1. The high frequency of healed linears in AT1 was observed over a 16-fold range in DNA concentration, indicating that small changes in DNA concentration do not affect the proportion of products in this assay. For each of the mutant plasmids, significant decreases in transformation frequency (1.5- to 3-fold) relative to AT1 were also found for linearized, but not circular, plasmids. Therefore, the decreases in healed linears, shown here, are minimal estimates.

33. We thank P. Carrico, S. Marglin, and L. Chen-Chiu for technical assistance; B. Rapkin for guidance with statistical analysis; S. Jinks-Robertson for providing plasmids; D. Gottschling for communicating results before publication; and H. Klein, A. Mitchell, M. A. Olsey, L. Sussel, M. Gwadz, B. Dunn, and E. B. Hoffman for critical comments. Supported by American Cancer Society grant MV-446 (to A.J.L.); by NIH grant GM 40094 and the Scarle Scholars' Program Chicago Community Trust (to D.S.); and by a postdoctoral fellowship from the Jane Coffin Childs Memorial Fund (to S.K.)

7 May 1990; accepted 10 August 1990

Protection of Mice Against the Lyme Disease Agent by Immunizing with Recombinant OspA

EROL FIKRIG, STEPHEN W. BARTHOLD, FRED S. KANTOR, RICHARD A. FLAVELL

Lyme borreliosis is a tick-borne illness caused by *Borrelia burgdorferi*. The gene for outer surface protein A (OspA) from *B. burgdorferi* strain N40 was cloned into an expression vector and expressed in *Escherichia coli*. C3H/HeJ mice actively immunized with live transformed *E. coli* or purified recombinant OspA protein produced antibodies to OspA and were protected from challenge with several strains of *B. burgdorferi*. Recombinant OspA is a candidate for a vaccine for Lyme borreliosis.

LYME DISEASE IS A MULTISYSTEM SPIROCHETAL illness characterized by rheumatologic, neurologic, cardiac, and dermatologic manifestations. The causative agent, *Borrelia burgdorferi*, is transmitted to humans mostly by *Ixodes* ticks (1). The host immune response to *B. burgdorferi* is incompletely understood; however, humoral immunity is important in protecting animals from infection. Passive immunization of hamsters with antiserum to *B. burgdorferi* prevents infection from intraperitoneal challenge with *B. burgdorferi* (2). The protection is partially strain-specific, however, because antiserum to *B. burgdorferi* strains from different geographic locations does not show full cross protection (3). Active immunization of hamsters with whole inactivated *B. burgdorferi* strain 297 prevents subsequent infection with *B. burgdorferi* strain 297 (4). The hamster model, however, is limited for the study of Lyme borreliosis because the animals do not develop clinical manifestations of Lyme disease.

A model of Lyme borreliosis has been developed in immunocompetent mice that resembles some of the clinical manifestations

of Lyme disease in humans (5). A strain of *B. burgdorferi*, designated N40, was isolated from Westchester County, New York; C3H/He mice infected with *B. burgdorferi* N40 develop spirochetemia 5 days after challenge and peak arthritis and carditis 14 days after infection. This model is useful for active immunization experiments with *B. burgdorferi* in contrast to the model of Lyme borreliosis in severe combined immunodeficiency mice (6).

We first verified that passive immunization is protective in the C3H/He mouse model. Mice were passively immunized with antiserum to *B. burgdorferi* N40 from mouse or rabbit and then challenged with *B. burgdorferi* N40 (7). Control groups were immunized with normal mouse or rabbit serum. After 5 or 14 days cultures of the blood and spleen were incubated for 2 weeks in Barbour-Stoenner-Kelly (BSK) medium (8). As expected from results in the hamster model, passive immunity was protective. Furthermore, the protective effect of rabbit serum was maintained at a dilution of 1:500. Protection extended to *B. burgdorferi* strain B31 and the clinical manifestations of disease at 14 days was prevented (Table 1).

The antigens responsible for eliciting the production of protective antibodies are not known; however, several outer surface proteins on *B. burgdorferi* are candidates. The outer membrane of *B. burgdorferi* is coated with a 31-kD protein known as outer surface protein A (OspA) (9), and a 34-kD protein named outer protein B (OspB) (10).

E. Fikrig, Section of Immunobiology, Yale University School of Medicine, and the Division of Infectious Diseases, Department of Internal Medicine, Yale University School of Medicine, New Haven, CT 06510.
S. W. Barthold, Section of Comparative Medicine, Yale University School of Medicine, New Haven, CT 06510.
F. S. Kantor, Division of Allergy and Clinical Immunology, Department of Internal Medicine, Yale University School of Medicine, New Haven, CT 06510.
R. A. Flavell, Section of Immunobiology and the Howard Hughes Medical Institute, Yale University School of Medicine, New Haven, CT 06510.